



Full paper/Mémoire

## A thienoquinoxaline and a styryl-quinoxaline as new fluorescent probes for amyloid- $\beta$ fibrils

Hanane Benzeid<sup>a,b,c</sup>, Emmanuelle Mothes<sup>a,b</sup>, El Mokhtar Essassi<sup>c</sup>, Peter Faller<sup>a,b,\*</sup>, Geneviève Pratviel<sup>a,\*,b</sup>

<sup>a</sup> CNRS, laboratoire de chimie de coordination (LCC), 205, route de Narbonne, 31077 Toulouse, France

<sup>b</sup> Université de Toulouse, UPS, INPT, LCC, 31077 Toulouse, France

<sup>c</sup> Laboratoire de chimie organique hétérocyclique, pôle de compétences pharmacochimie, université Mohammed V-Agdal, faculté des sciences, avenue Ibn Battouta, BP 1014, Rabat, Morocco

## ARTICLE INFO

## Article history:

Received 5 May 2011

Accepted after revision 20 October 2011

Available online 13 December 2011

## Keywords:

A $\beta$ -peptide

Fibrils

Fluorescent staining

Lysozyme

Quinoxaline

## ABSTRACT

Simple and easy to prepare quinoxaline derivatives proved able to stain amyloid fibers such as aggregated lysozyme and A $\beta$ (1–40)-peptide by a fluorescence “turn on” mechanism. Thienoquinoxaline **1** allowed the detection of lysozyme and A $\beta$ (1–40) fibers at  $\lambda = 555$  and  $532$  nm, respectively, with excitation at  $\lambda = 450$  nm. Styryl-quinoxaline **2** stained lysozyme and A $\beta$ (1–40) fibers with fluorescence at  $\lambda = 579$  and  $567$  nm, respectively, upon excitation at  $\lambda = 453$  nm. The apparent  $K_d$  values for A $\beta$ (1–40) fibers were  $77$  and  $294$  nM for **1** and **2**, respectively. The sensitivity of the aggregates detection assay with these new dyes was higher than that of thioflavin T. Considering their unique fluorescence properties compared to other dyes reported in the field, they can be considered as additional staining tools for the detection and studies of peptide/protein aggregation.

© 2011 Académie des sciences. Published by Elsevier Masson SAS. All rights reserved.

### 1. Introduction

The development of markers for fibrillar aggregates and prefibrillar structures is an extremely active research field due to the involvement of peptide or protein aggregation in neurodegenerative diseases including prion, Parkinson's, Huntington's and Alzheimer's disease [1,2]. In each disease, a different protein is implicated. Finding amyloid imaging agents for different aggregation states as well as different peptide/protein aggregates depending on the nature of the peptide/protein is crucial in order to afford tools for monitoring fibrils formation *in vitro* and *in vivo*. They would provide the means for a better understanding of neurodegenerative disorders, and would afford agents for early diagnosis. Thus, molecular probes that specifically target protein/peptide aggregates and allow *in vitro* and

*in vivo* imaging of these pathological hallmarks, are of great importance. Moreover, in a more general context, a variety of convenient analytical tools for the (kinetic, structural... ) studies of protein misfolding processes leading to aggregation and/or fibrillation would be useful [3].

Among the various imaging methodologies (MRI, PET, radiolabel) [4–8], fluorescent dyes are attractive since they are inexpensive and sensitive. They are extensively used for *in vitro* and *ex vivo* staining of amyloids. *In vivo* near-infrared imaging offers the advantage of a noninvasive operation that does not require expensive instrumentation. Hence, the fluorescent staining of amyloids has greatly evolved during the last decade.

The early dye Thioflavin T (ThT) [9–12] is still widely used as detection agents for amyloids. ThT is a blue-emission dye ( $\lambda_{\max(\text{em})} \sim 480$  nm). Non charged analogues of ThT have been prepared for better blood–brain barrier crossing yet are endowed with similar blue fluorescence properties [10,13–15]. Congo Red analogue reached a green fluorescence ( $\lambda_{\max(\text{em})} \sim 550$  nm) [16,17] as well as pentameric thiophene derivatives ( $\lambda_{\max(\text{em})} = 550$  nm)

\* Corresponding authors.

E-mail addresses: peter.faller@lcc-toulouse.fr (P. Faller), genevieve.pratviel@lcc-toulouse.fr (G. Pratviel).

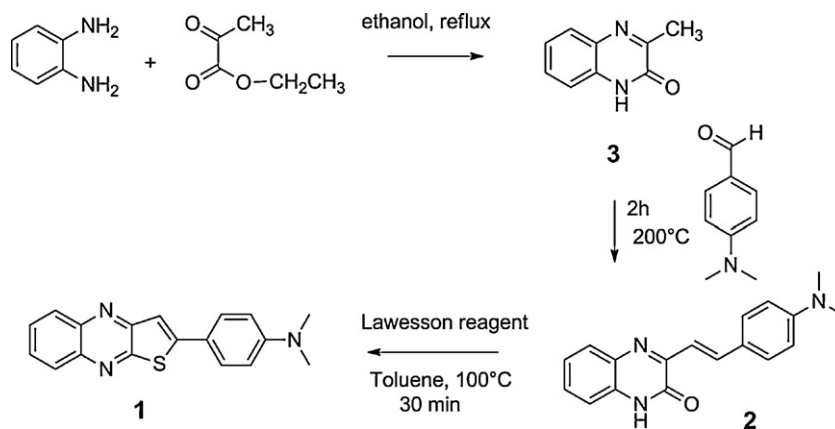


Fig. 1. Synthesis of quinoxalines.

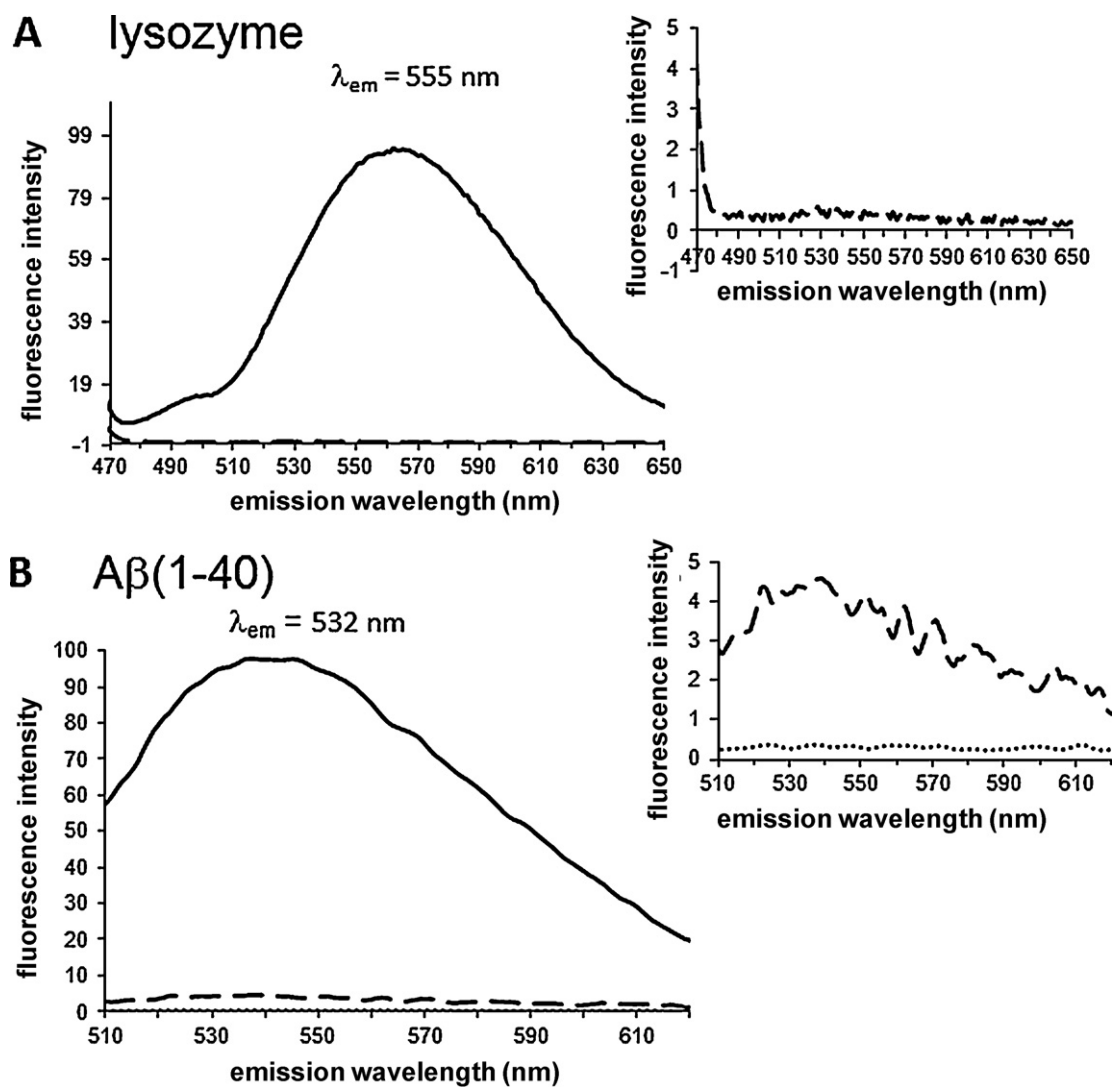


Fig. 2. Fluorescence “turn on” of **1** induced by aggregates of lysozyme (A) and A $\beta$ (1-40) (B). Compound **1** (3  $\mu\text{M}$ ) was incubated in the presence of 6  $\mu\text{M}$  of aggregated material (solid line), 6  $\mu\text{M}$  of non aggregated material (dashed line), and in the buffer (dotted line). Emission spectra were recorded in 20 mM phosphate buffer pH = 7.4, NaCl 100 mM (DMSO 0.5% in A and 0.8% in B) with  $\lambda_{ex} = 450 \text{ nm}$ .

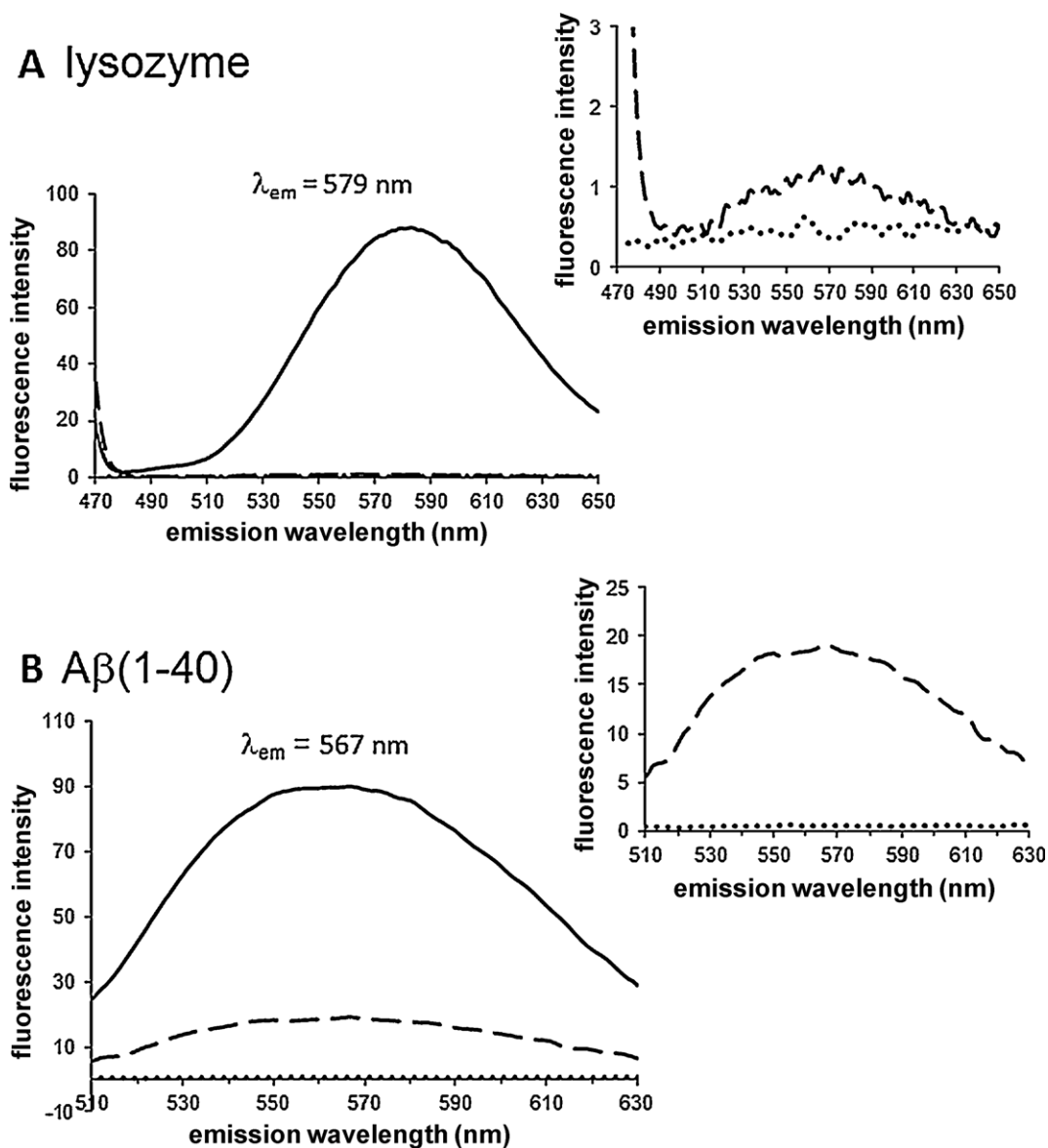


Fig. 3. Fluorescence “turn on” of **2** induced by aggregates of lysozyme (A) and A $\beta$ (1–40) (B). Compound **2** (3  $\mu$ M) was incubated in the presence of 6  $\mu$ M of aggregated material (solid line), 6  $\mu$ M of non aggregated material (dashed line), and in the buffer (dotted line). Emission spectra were recorded in 20 mM phosphate buffer pH = 7.4, NaCl 100 mM (DMSO 0.5% in A and 0.8% in B) with  $\lambda_{ex}$  = 453 nm.

[12]. Polythiophenes [18], bis-thiophene derivative NIAD-4 [19] ( $\lambda_{max(em)}$  = 600 nm) and styryl derivative 2C40 ( $\lambda_{max(em)}$  = 650 nm) exhibit a red fluorescence [20]. Further red-shifting of spectral characteristics afforded potential near-infrared fluorescent probes such as oxazine derivative AOI987 [21], and curcumin derivative CRANAD-2 ( $\lambda_{max(em)}$  = 700 nm) compatible with in vivo use [22].

Recently, morphologically distinct fibrillar deposits could be resolved with luminescent conjugated polythiophenes [18,23], or Nile red dye [24], and early fibrillation states could be detected by fluorescence quenching effect with TROL dye or by fluorescence enhancement with pentameric thiophene p-FTAA ( $\lambda_{max(em)}$   $\sim$  550 nm) [25,26].

In the present work, we report on convenient novel tools for amyloid staining consisting of quinoxaline derivatives that are essentially nonfluorescent in aqueous buffers and exhibit a yellow fluorescence ( $\lambda_{max(em)}$   $\sim$  530–580 nm,  $\lambda_{max(ex)}$  = 468 nm) when bound to amyloid fibers such as lysozyme and A $\beta$ (1–40)-peptide aggregates.

## 2. Results and discussion

Quinoxaline derivatives **1–3** were prepared by simple procedure. Condensation of *o*-phenylenediamine and ethyl pyruvate led to quinoxaline **3**, which was reacted with 4-*N,N'*-dimethylbenzaldehyde to give styryl quinoxaline **2**.

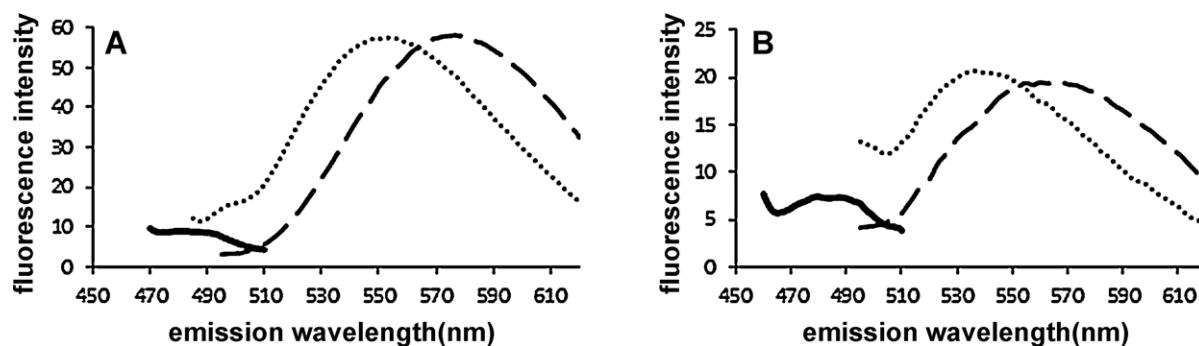


Fig. 4. Emission spectra of **1** (3  $\mu\text{M}$ , dotted line), **2** (3  $\mu\text{M}$ , dashed line), and ThT (3  $\mu\text{M}$ , solid line) incubated separately with 6  $\mu\text{M}$  aggregated lysozyme (A) and A $\beta$ (1–40) (B) in 20 mM potassium phosphate buffer, NaCl 100 mM (DMSO 0.5%) pH 7.4.  $\lambda_{\text{ex}} = 440$  nm for ThT, and 468 nm for **1** and **2**. Emission bandpass = 10 nm, excitation bandpass = 10 nm.

Thienoquinoxaline **1** was obtained from **2** in the presence of Lawesson's reagent (Fig. 1).

The two compounds were soluble in DMSO with molar extinction coefficients of 30 900  $\text{M}^{-1} \text{cm}^{-1}$  at 450 nm and 26 700  $\text{M}^{-1} \text{cm}^{-1}$  at 453 nm for **1** and **2**, respectively. They exhibited bright fluorescence in DMSO while the aqueous solutions only have trace emission. In DMSO, both dyes showed the same fluorescence emission  $\lambda_{\text{max(em)}} = 600$  nm and excitation maxima  $\lambda_{\text{max(ex)}} = 468$  nm (Stokes shift = 132 nm). The spectra are provided as Supplementary Information (Appendix A: Figs. S1 and S2). The compounds were stable under irradiation conditions used in this study, i.e. less than 3 min.

Considering structural analogy with thioflavin T (ThT) or its non charged benzothiazole analogues [10,14], and CRANAD-2 [22], that can be used as probes for amyloid fibrils, **1** and **2** were assessed for their suitability as new probes for two types of fibrils, the aggregated states of A $\beta$ (1–40) peptide and lysozyme from chicken egg white.

When added to suspensions of A $\beta$ (1–40) and lysozyme (6  $\mu\text{M}$ ) previously exposed to conditions causing aggregation, both **1** (Fig. 2) and **2** (Fig. 3) (3  $\mu\text{M}$ ) exhibited fluorescence in 20 mM phosphate buffer pH 7.4 and NaCl 100 mM. Weak fluorescence response was observed if the dye was alone in buffer or if the peptide was not in an aggregated form (Fig. 2 for **1**) (Fig. 3 for **2**). In the presence of both aggregated lysozyme and A $\beta$ (1–40) the fluorescence of **1** is "turned on" with a > 100-fold fluorescence intensity increase. The  $\lambda_{\text{max(em)}}$  were observed at 555 and 532 nm for aggregated lysozyme and A $\beta$ (1–40), respectively, upon irradiation at 450 nm. The binding of

compound **2** to aggregated lysozyme and A $\beta$ (1–40) is also accompanied by a dramatic enhancement of the fluorescence emission,  $\lambda_{\text{max(em)}} = 579$  and 567 nm, respectively upon excitation of the dye at 453 nm. The ratio between the fluorescence intensity in the presence and in the absence of fibrils was  $\sim 90$  for both lysozyme and A $\beta$ (1–40). A residual fluorescence was noted when the dyes were incubated with non aggregated A $\beta$ (1–40) (dashed line Fig. 2B and dotted line Fig. 3B) due to partial aggregation of the peptide. The control in the absence of peptide material was fluorescence negative (Fig. 2 and Fig. 3).

The fluorescence spectra of Figs. 2 and 3 were obtained with excitation wavelength corresponding to the absorbance maximum of each compound, namely 453 and 450 nm for **1** and **2**, respectively. However, fluorescence excitation spectra of both compounds in interaction with both fibrillar targets show the same  $\lambda_{\text{max(ex)}} = 468$  nm (not shown). Slightly higher fluorescence intensity is observed ( $\sim 25\%$  increase) when  $\lambda_{\text{ex}} = 468$  nm is used instead of  $\lambda_{\text{ex}} = 450$  (or 453) nm. The sensitivity of compounds **1** and **2** with respect to ThT in amyloid fibers detection assay was compared (Fig. 4). Compounds **1** and **2** were ca 6- and 3-fold more sensitive than ThT for the detection of lysozyme and A $\beta$ (1–40)-peptide aggregate, respectively.

Fluorescence became more intense with increasing concentrations of dyes as illustrated in Fig. 5 in the case of interaction with A $\beta$ (1–40) aggregates. From these titration experiments the apparent binding affinity constant of the two compounds with aggregated A $\beta$ (1–40) peptide were calculated (Appendix A: Fig. S3). For comparison

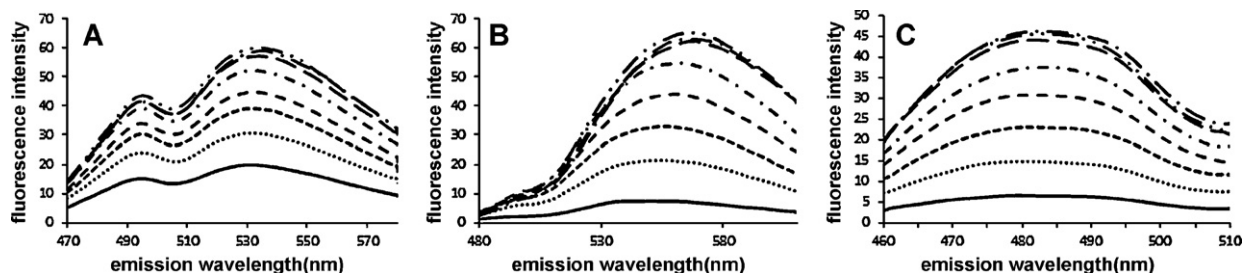


Fig. 5. Emission spectra of increasing concentrations of **1**: 0 to 2.5  $\mu\text{M}$  (A), **2**: 0 to 6.6  $\mu\text{M}$  (B), and ThT: 0 to 10  $\mu\text{M}$  (C) incubated with aggregated A $\beta$ (1–40) peptide 6  $\mu\text{M}$  in 20 mM potassium phosphate buffer pH 7.4, NaCl 100 mM.  $\lambda_{\text{ex}} = 440$  nm, bandpass = 10 nm and emission bandpass = 10 nm.

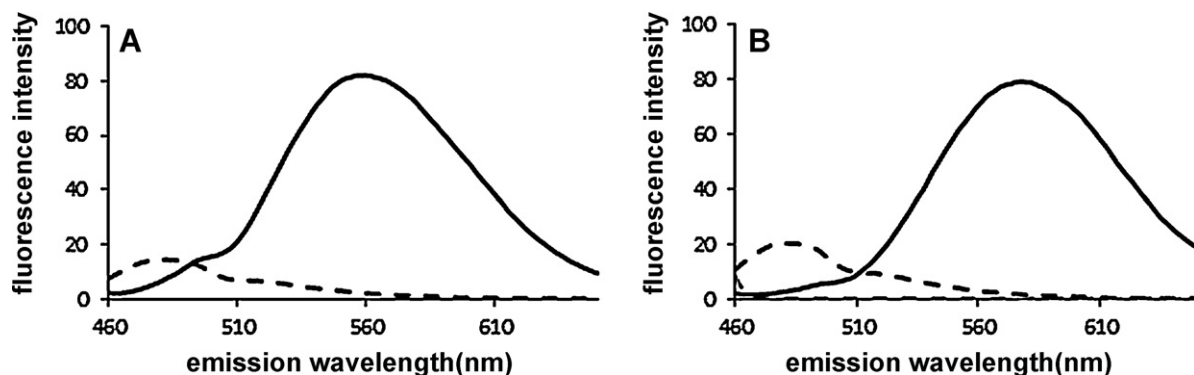


Fig. 6. Emission spectra of ThT (3  $\mu\text{M}$ ) bound to aggregated lysozyme (6  $\mu\text{M}$ ) (dashed line) and in the presence of competitor **1** (3  $\mu\text{M}$ ) (A) and **2** (3  $\mu\text{M}$ ) (B) (solid line). Emission bandpass = 10 nm.  $\lambda_{\text{ex}}$  = 440 nm, bandpass = 10 nm.

purpose ThT was also tested separately under the same experimental conditions. The apparent dissociation constant of **1** ( $K_d = 77 \pm 17$  nM) and **2** ( $K_d = 294 \pm 90$  nM) was lower than that of ThT ( $K_d = 925 \pm 30$  nM). The  $K_d$  of ThT was in accordance with previous data [9,10]. The  $K_d$  is slightly higher than the apparent  $K_d = 20$  nM of the fluorophore K114, which is used as a cell permeable amyloid staining dye and works on the same principle, i.e. it is not soluble in buffer but binds to amyloid fibrils [17]. Since, three classes of binding sites have been evidenced on A $\beta$ (1–40) peptide [13,27], it would be interesting to know whether the new compounds show competitive or independent binding with respect to ThT. Unfortunately, it is not possible to determine whether **1** and **2** are able to displace ThT bound to A $\beta$ (1–40) through competition experiments monitoring the decrease of the fluorescence of bound ThT upon addition of increasing concentration of competitor dye. The fluorescence spectra of **1** and ThT overlap in the 470–500 nm window of emission as well as in the excitation window. The low fluorescence emission of **2** in the same emission window also biased the assay. On the other hand, equimolar quantity of **1** and/or **2** turned off the fluorescence of lysozyme/ThT complex after 5 min with concomitant exhibition of their own typical fluorescence (Fig. 6). However, in this case as well, it is not possible to ascertain the competitive binding of the small molecules to the same site in fibrils since the fluorescence of bound ThT might be quenched by **1** and **2** (FRET).

Interestingly, compound **1** and **2** turned on the fluorescence upon interaction with fibrils as is the case for ThT, but in contrast to ThT, **1** and **2** showed a blue shift in emission (Appendix A: Figs. S1 and S2). As the origin of the shift in ThT is still under discussion [11,28–31], the behavior of **1** and **2** is more classical, and can be explained by the lower stabilisation of the dipolar moment due to the more apolar environment of **1** and **2** in the amyloid fibrils compared to the solvent [32]. In a more apolar environment, the electron-vibrational coupling between the fluorophore and the solvent is reduced which leads to a lower displacement parameter and hence the observed blue shift for emission. Furthermore, the fluorescence of the two dyes in complex with fibrils showed some variations depending on the nature of the tested aggregated model (Table 1). The maximum of fluorescence emission of the lysozyme staining appeared always at higher wavelength compared to A $\beta$ (1–40) amyloid for each dyes. As a consequence the blue shift is higher in the A $\beta$ (1–40) environment compared to lysozyme:  $\lambda_{\text{max}} = 532$  nm (A $\beta$ ) vs 555 nm (lysozyme) for **1**, and  $\lambda_{\text{max}} = 567$  nm (A $\beta$ ) vs 579 nm (lysozyme) for **2**. The larger blue shift of **1** and **2** bound to A $\beta$ (1–40) amyloid can be explained by a more apolar binding site compared to lysozyme. Additionally, the fluorescence blue shift exhibited by **1** when bound to fibrils is always more important than that of **2**, which may be related to the more rigid aromatic structure of **1**. The reason is not known, but could be explained by a more polar excited state of **1** compared to **2**.

Table 1

Fluorescence maximum  $\lambda_{\text{max}}$  (nm) of free dyes and dyes in complex with aggregated material.

	DMSO	Buffer	A $\beta$ (1–40) fibrils	Lysozyme
<b>1</b>				
Excitation	468	–	468	468
Emission	600	–	(495 and) 532	555
<b>2</b>				
Excitation	468	–	468	468
Emission	600	–	567	579
ThT				
Excitation		385	450	450
Emission		445	482	482

### 3. Conclusion

New quinoxaline derivatives (**1** and **2**) proved able to stain amyloid fibers such as aggregated lysozyme and A $\beta$ (1–40)-peptide with fluorescence detection at  $\lambda \sim 530$ –580 nm and excitation at  $\lambda \sim 450$  nm. The apparent  $K_d$  values for aggregated A $\beta$ (1–40) were 77 nM and 294 nM for **1** and **2**, respectively. The main interest of these compounds in the staining of peptide aggregates is (i) their fluorescence “turn on” with a ca 100-fold increase of fluorescence upon binding to amyloids, which makes them sensitive tools, (ii) the large difference between excitation and emission wavelength in the complex (> 100 nm) associated with emission at high

wavelength (> 530 nm), (iii) their high affinity for fibrils and, (iv) in contrast to ThT, their different emission properties when in complex with distinct types of fibrils. In summary, since their fluorescent properties are different from other available markers, compounds **1** and **2** afford supplementary staining tools for amyloid fibers detection.

## 4. Experimental

### 4.1. Materials

Thioflavin T (C.I. 49005, basic yellow 1), *o*-phenylenediamine and Lawesson's reagent were purchased from Acros. Ethyl pyruvate and 4-(dimethylamino)benzaldehyde were from Aldrich. All the solutions were prepared using milliQ water. Dimethyl sulfoxide (analysis grade) was purchased from Merck. Buffers and lysozyme from chicken egg white (molecular weight 13 930 Da, molar extinction coefficient  $3.65 \times 10^4 \text{ M}^{-1} \cdot \text{cm}^{-1}$ ) were purchased from Sigma-Aldrich. Synthetic A $\beta$  (1–40) peptide (sequence: DAEFRHDSGYEVHHQKLVFFAEDVGSNKGAIIGLMVGGVV) was obtained from GeneCust (Dudelange, Luxembourg) and was used without further purification. All experiments were performed in 20 mM potassium phosphate buffer pH 7.4, NaCl 100 mM, and conducted at room temperature. Thienoquinoxaline (**1**) and styryl-quinoxaline (**2**) were not water-soluble. They were dissolved in DMSO and added to the samples as concentrated solutions (final DMSO 0.2 to 3%).

### 4.2. Synthesis of quinoxaline 3

Condensation of *o*-phenylenediamine (1 g, 9.25 mmol) and ethyl pyruvate (1.03 mL, 9.25 mmol) was performed in 10 mL of 4 N HCl solution during 15 min at ambient temperature. After filtration of the reaction medium the product was washed with distilled water until neutral filtrate was obtained. The solid was dried under vacuum. Yield: 1.18 g (7.4 mmol, 80%) white solid.  $^1\text{H}$  NMR (300 MHz,  $d_6$ -DMSO)  $\delta$  12.30 (s, 1H, NH), 7.68 (d, 1H, H<sub>Ar</sub>), 7.46 (m, 1H, H<sub>Ar</sub>), 7.25 (m, 2H, H<sub>Ar</sub>), 2.40 (s, 3H, CH<sub>3</sub>).  $^{13}\text{C}$  NMR (63 MHz,  $d_6$ -DMSO)  $\delta$  159.7, 155.4, 132.4, 132.1 (C<sub>q</sub>), 129.7, 128.3, 123.5, 115.7 (C<sub>Ar</sub>), 21.0 (CH<sub>3</sub>). Elemental analysis (%) calcd for C<sub>9</sub>H<sub>8</sub>N<sub>2</sub>O: C 67.49, H 5.03, N 17.49; found: C 67.45, H 5.49, N 17.50. Positive FAB-MS (MNBA)  $m/z$  (M + H)<sup>+</sup> 161. UV-vis (DMSO)  $\lambda_{\text{max}}$  nm ( $\epsilon \text{ M}^{-1} \text{ cm}^{-1}$ ) 340 (3 000), 332 (3 000), 280 (2 400).

Synthesis of (*E*)-3-(4-(dimethylamino)styryl)quinoxaline-2-one or styryl-quinoxaline (**2**). Compound **2** was prepared by condensation of quinoxaline **3** (1 g, 6.25 mmol) with 4-*N,N'*-dimethylbenzaldehyde (1.8 g, 12.5 mmol) for 2 h at 200 °C. The reaction mixture was allowed to cool down. The crude product was taken in ethanol (50 mL), heated at 100 °C for 10 min, filtrated. The solid was washed with ethanol and dried under vacuum. Yield 1.02 g (5.3 mmol, 85%) yellow solid.  $^1\text{H}$  NMR (250 MHz,  $d_6$ -DMSO)  $\delta$  12.38 (s, 1H, NH), 7.99 (d, 1H, CH<sub>C=C</sub>,  $^3J = 16$  Hz), 7.73 (dd, 1H, H<sub>Ar</sub>,  $^3J = 8.7$  Hz), 7.58 (d, 2H, H<sub>Ar</sub>,  $^3J = 8.8$  Hz), 7.43 (m, 2H, H<sub>Ar</sub>), 7.38 (d, 1H, CH<sub>C=C</sub>,  $^3J = 16$  Hz), 7.29 (m, 2H, H<sub>Ar</sub>), 6.79 (d, 2H,  $^3J = 8.7$  Hz), 3.00 (s, 6H, 2CH<sub>3</sub>).  $^{13}\text{C}$  NMR (75.5 MHz,  $d_6$ -DMSO)  $\delta$  155.4,

154.0, 151.6, 138.3, 133.1, 131.7, 129.7 (2xC), 129.3, 128.3, 124.1, 123.8, 116.6, 115.6, 112.6 (2xC), 40.2 (2xC). Elemental analysis (%) calcd for C<sub>18</sub>H<sub>17</sub>N<sub>3</sub>O·0.4CH<sub>3</sub>CH<sub>2</sub>OH: C 72.89, H 6.31, N 13.56; found: C 72.75, H 6.32, N 14.13. Positive ESI-MS  $m/z$  (M + H)<sup>+</sup> 292.4. UV-vis (DMSO)  $\lambda_{\text{max}}$  nm ( $\epsilon \text{ M}^{-1} \text{ cm}^{-1}$ ) 453 (26 700). F(°C) 264.

Synthesis of *N,N*-dimethyl-4-(thieno[2,3-*b*]quinoxaline-2-yl)aniline or quinoxaline (**1**). Compound **2** (1 g, 3.43 mmol) in toluene was refluxed with Lawesson's reagent (1.4 g, 3.43 mmol) for 30 min. The solvent was evaporated. The crude solid was taken in hot ethanol, filtered, washed with ethanol. The solid was dried under vacuum. Yield: 0.73 g (2.4 mmol, 70%) brown solid.  $^1\text{H}$  NMR (300 MHz,  $d_6$ -DMSO)  $\delta$  8.09–8.13 (m, 2H), 7.89 (s, 1H, H), 7.83 (d, 2H, H<sub>qNMe2</sub>,  $^3J = 9$  Hz), 7.82 (m, 2H), 6.86 (d, 2H, H<sub>qNMe2</sub>,  $^3J = 9$  Hz).  $^{13}\text{C}$  NMR (75.5 MHz, CDCl<sub>3</sub>)  $\delta$  157.0, 153.7, 152.7, 151.8, 141.1, 139.7, 129.0, 128.8, 128.4, 128.3, 128.1(2xC), 120.7, 113.0, 112.0(2xC), 40.2(2xC). Elemental analysis (%) calcd for C<sub>18</sub>H<sub>15</sub>N<sub>3</sub>S·0.8CH<sub>3</sub>CH<sub>2</sub>OH: C 68.78, H 5.83, N 12.28; found: C 68.44, H 5.20, N 12.35. Positive FAB (MNBA)  $m/z$  (M + H)<sup>+</sup> 306. UV-vis (DMSO)  $\lambda_{\text{max}}$  nm ( $\epsilon \text{ M}^{-1} \text{ cm}^{-1}$ ) 450 (30 900), 312 (14 800). F(°C) 260.

### 4.3. Preparation of amyloid fibrils of lysozyme from chicken egg white

Lysozyme (2 mg/mL, 143  $\mu\text{M}$ ) was incubated in 100 mM glycine buffer pH = 2.5, NaN<sub>3</sub> 0.02% at 57 °C upon stirring (thermomixer) during 10 days. After aggregation (evidenced by Thioflavin T fluorimetric assay) [33] the aggregated lysozyme solution was stored at –20 °C for several weeks. Before tests an aliquot was diluted in 20 mM phosphate buffer pH = 7.4, NaCl 100 mM and the pH adjusted with concentrated NaOH solution. Final lysozyme concentration was 12  $\mu\text{M}$ .

### 4.4. Preparation of A $\beta$ (1–40) fibrils

Peptide A $\beta$ (1–40) was dissolved in 25 mM sodium hydroxide solution, pH = 12.0 (~ 4 mg/mL). One volume of this initial solution was diluted with 3 volumes of 10 mM phosphate buffer pH = 7.4, NaCl 100 mM, NaN<sub>3</sub> 0.02%. The pH was adjusted to 7.4 with concentrated HCl. The peptide concentration was measured by UV-vis spectrometry taking the molar extinction coefficient of tyrosine at 276 nm ( $\epsilon = 1410 \text{ M}^{-1} \text{ cm}^{-1}$ ). Concentrations of A $\beta$ (1–40) was 273  $\mu\text{M}$ . Aggregation of A $\beta$ (1–40) was allowed to proceed upon incubation at 30 °C for 21 days. After aggregation (evidenced by Thioflavin T fluorimetric assay) [33] aggregated peptide solutions was stored at –20 °C for several weeks.

### 4.5. Non-aggregated material

Non-aggregated material consisted of freshly prepared solutions. Lysozyme was dissolved in 20 mM phosphate buffer pH = 7.4, NaCl 100 mM and A $\beta$ (1–40) in 25 mM sodium hydroxide solution, pH = 12.0. Further dilutions with 20 mM phosphate buffer pH = 7.4, NaCl 100 mM were prepared and pH adjusted to 7.4 with HCl and used.

#### 4.6. Compounds preparation

Compounds **1** and **2** were prepared as 2 mM stock solution in DMSO. Suitable DMSO solutions of dyes were directly added into the assay buffer so that the maximum final DMSO content in the assays was 0.2 to 2%. Stock solution of ThT was prepared in H<sub>2</sub>O.

#### 4.7. Fluorescence binding assay

Fluorescence intensity changes associated with ligand binding to lysozyme and A $\beta$ (1–40) were recorded in a Safas FLX-Xenius fluorimeter (cuvette and plate reader). Dye binding assay were performed at a fixed 6  $\mu$ M aggregated (or non-aggregated) material (lysozyme or A $\beta$ ), diluted from the stock solution into 200  $\mu$ L (plate) or 500  $\mu$ L (cuvette) of 20 mM phosphate buffer pH = 7.4, 100 mM NaCl. Concentrated DMSO solutions of dyes were added for increasing concentration of ligand until a plateau was reached. In plates the % of DMSO was constant (0.5%). In cuvette experiments the DMSO content varied from 0 to 2%. Measurements with ThT, compound **1** and compound **2** utilized  $\lambda_{\text{ex}}$  = 440, 450, and 453 nm, respectively, 10 nm bandpass. Emission were recorded at  $\lambda_{\text{em(max)}}$  = 480 nm (ThT), 535 nm (compound **1**), and 560 nm (compound **2**), 10 nm bandpass. Excitation wavelength is indicated in the Figure legends. Experiments were conducted at room temperature. The K<sub>d</sub> binding curves were generated by software Kaleidagraph with non linear one site binding regression. Measurements were carried out after 5 min of incubation of dye with aggregated material. Longer incubation times did not result in higher fluorescence.

#### Acknowledgements

This work was partly supported by the International Associated Moroccan-French Laboratory on Molecular Chemistry (LIA, LCMMF). We would like to thank Dr. Neil Johnson, IPBS Toulouse, for helpful discussions.

#### Appendix A. Supplementary data

Supplementary data associated with this article can be found, in the online version, at [doi:10.1016/j.crci.2011.10.009](https://doi.org/10.1016/j.crci.2011.10.009).

#### References

- [1] F. Chiti, C.M. Dobson, *Annu. Rev. Biochem.* 75 (2006) 333.
- [2] M. Lindgren, P. Hammarstrom, *FEBS J.* 277 (2010) 1380.
- [3] A. Hawe, M. Sutter, W. Jiskoot, *Pharm. Res.* 25 (2008) 1487.
- [4] A. Nordberg, *Lancet Neurol.* 3 (2004) 519.
- [5] M. Higuchi, N. Iwata, Y. Matsuba, K. Sato, K. Sasamoto, T.C. Saido, *Nat. Neurosci.* 8 (2005) 527.
- [6] C.A. Mathis, B.J. Lopresti, W.E. Klunk, *Nucl. Med. Biol.* 34 (2007) 809.
- [7] L. Cai, R.B. Innis, V.W. Pike, *Curr. Med. Chem.* 14 (2007) 19.
- [8] P.W. Thompson, A. Lockhart, *Drug Discov. Today* 14 (2009) 241.
- [9] H. LeVine 3rd, *Protein Sci.* 2 (1993) 404.
- [10] W.E. Klunk, Y. Wang, G.F. Huang, M.L. Debnath, D.P. Holt, C.A. Mathis, *Life Sci.* 69 (2001) 1471.
- [11] L.S. Wolfe, M.F. Calabrese, A. Nath, D.V. Blaho, A.D. Miranker, Y. Xiong, *Proc. Natl. Acad. Sci. U S A* 107 (2010) 16863.
- [12] A. Aslund, C.J. Sigurdson, T. Klingstedt, S. Grathwohl, T. Bolmont, D.L. Dickstein, E. Glimsdal, S. Prokop, M. Lindgren, P. Konradsson, D.M. Holtzman, P.R. Hof, F.L. Heppner, S. Gandy, M. Jucker, A. Aguzzi, P. Hammarstrom, K.P. Nilsson, *ACS Chem. Biol.* 4 (2009) 673.
- [13] A. Lockhart, L. Ye, D.B. Judd, A.T. Merritt, P.N. Lowe, J.L. Morgenstern, G. Hong, A.D. Gee, J. Brown, *J. Biol. Chem.* 280 (2005) 7677.
- [14] R. Leuma Yona, S. Mazeris, P. Faller, E. Gras, *ChemMedChem* 3 (2008) 63.
- [15] M.C. Hong, Y.K. Kim, J.Y. Choi, S.Q. Yang, H. Rhee, Y.H. Ryu, T.H. Choi, G.J. Cheon, G.I. An, H.Y. Kim, Y. Kim, D.J. Kim, J.S. Lee, Y.T. Chang, K.C. Lee, *Bioorg. Med. Chem.* 18 (2010) 7724.
- [16] D.M. Skovronsky, B. Zhang, M.P. Kung, H.F. Kung, J.Q. Trojanowski, V.M. Lee, *Proc. Natl. Acad. Sci. U S A* 97 (2000) 7609.
- [17] H. LeVine 3rd, *Biochemistry* 44 (2005) 15937.
- [18] C.J. Sigurdson, K.P. Nilsson, S. Hornemann, G. Manco, M. Polymenidou, P. Schwarz, M. Leclerc, P. Hammarstrom, K. Wuthrich, A. Aguzzi, *Nat. Methods* 4 (2007) 1023.
- [19] E.E. Nesterov, J. Skoch, B.T. Hyman, W.E. Klunk, B.J. Bacskai, T.M. Swager, *Angew. Chem. Int. Ed.* 44 (2005) 5452.
- [20] Q. Li, J.S. Lee, C. Ha, C.B. Park, G. Yang, W.B. Gan, Y.T. Chang, *Angew. Chem. Int. Ed.* 43 (2004) 6331.
- [21] M. Hintersteiner, A. Enz, P. Frey, A.L. Jatón, W. Kinzy, R. Kneuer, U. Neumann, M. Rudin, M. Staufenberg, M. Stoeckli, K.H. Wiederhold, H.U. Gremlich, *Nat. Biotechnol.* 23 (2005) 577.
- [22] C. Ran, X. Xu, S.B. Raymond, B.J. Ferrara, K. Neal, B.J. Bacskai, Z. Medarova, A. Moore, *J. Am. Chem. Soc.* 131 (2009) 15257.
- [23] K.P. Nilsson, A. Aslund, I. Berg, S. Nystrom, P. Konradsson, A. Herland, O. Inganas, F. Stabo-Eeg, M. Lindgren, G.T. Westermark, L. Lannfelt, L.N. Nilsson, P. Hammarstrom, *ACS Chem. Biol.* 2 (2007) 553.
- [24] R. Mishra, D. Sjolander, P. Hammarstrom, *Mol. Biosyst.* 7 (2011) 1232.
- [25] A.A. Reinke, G.A. Abulwerdi, J.E. Gestwicki, *Chembiochem* 11 (2010) 1889.
- [26] P. Hammarstrom, R. Simon, S. Nystrom, P. Konradsson, A. Aslund, K.P. Nilsson, *Biochemistry* 49 (2010) 6838.
- [27] L. Ye, J.L. Morgenstern, A.D. Gee, G. Hong, J. Brown, A. Lockhart, *J. Biol. Chem.* 280 (2005) 23599.
- [28] H. LeVine 3rd, *Methods Enzymol.* 309 (1999) 274.
- [29] V.I. Stsiapura, A.A. Maskevich, V.A. Kuzmitsky, V.N. Uversky, I.M. Kuznetsova, K.K. Turoverov, *J. Phys. Chem. B* 112 (2008) 15893.
- [30] M. Biancalana, S. Koide, *Biochim. Biophys. Acta* 1804 (2010) 1405.
- [31] E.S. Voropai, M.P. Samtsov, K.N. Kaplevskii, A.A. Maskevich, V.I. Stepuro, O.I. Povarova, I.M. Kuznetsova, K.K. Turoverov, A.L. Fink, V.N. Uverskii, *J. Appl. Spect.* 70 (2003) 868.
- [32] J.B. Birks, *Photophysics of aromatic molecules*, Wiley-Interscience, London, New York, 1970.
- [33] M.R. Nilsson, *Methods* 34 (2004) 151.